

First-principles study on magnetism of Fe-rich Nd(Fe,Ga) alloys existing in grain boundary phases in Ga doped Nd-Fe-B magnets

Kazushige Hyodo and Akimasa Sakuma

Department of Applied Physics, Tohoku University, Aoba 6-6-05, Aoba-ku, Sendai 980-8579, Japan

Yuta Toga

ESICMM, National Institute of Materials Science, Sengen 1-2-1, Tsukuba 305-0047, Japan

We studied the magnetic properties of Fe-rich Nd(Fe,Ga) alloys, which appear in grain boundary (GB) phase of Ga doped Nd-Fe-B magnets, focusing on the effects of structure change from amorphous to ordered phase and the presence of Ga doping. To examine the stable magnetic structures of these alloys, first-principles calculations were performed for Fe-rich amorphous $\text{Nd}_{30}\text{Fe}_{70-x}\text{Ga}_x$ and crystalline ordered $\text{Nd}_6\text{Fe}_{14-x}\text{Ga}_x$ systems. The amorphous system shows a ferromagnetic state and its magnetism is little influenced by Ga doping. In contrast, in the ordered $\text{Nd}_6\text{Fe}_{14-x}\text{Ga}_x$, slight Ga doping ($x = 1$) was found to significantly contribute to stabilizing an anti-ferromagnetic state, which is expected to prevent the domain walls passing across the GBs in Nd-Fe-B magnets.

I. INTRODUCTION

Higher performance of Nd-Fe-B permanent magnets is desired for realizing more-energy-efficient motors. Especially, for motors in electric vehicles operating under high temperature, larger coercive force (H_c) for suppressing thermal fluctuation of magnetization is strongly required. However, even in recent Nd-Fe-B magnets, the value of achieved H_c is only $\sim 20\%$ compared with the ideal value. To remedy some of the causes of the decline of H_c , many studies have focused on trying to optimize the internal structures in Nd-Fe-B, where fine $\text{Nd}_2\text{Fe}_{14}\text{B}$ grains and a few other phases exist. One idea focuses on the nucleation effect in the $\text{Nd}_2\text{Fe}_{14}\text{B}$ grains, which will decrease H_c , and attempts have been made to reduce the grain size^{1,2}.

As well as the above approach, these days, pinning effects of domain walls (DWs) at the grain boundary (GB) phases of $\text{Nd}_2\text{Fe}_{14}\text{B}$ become other attractive strategy. Executions of optimized post-sintered annealing were found to produce continuous thin GB layers, whose width is $\simeq 3\text{nm}$, along the $\text{Nd}_2\text{Fe}_{14}\text{B}$ grains.³⁻⁶ Although this GB phase involves an Fe-rich amorphous alloy ($\sim \text{Nd}_{30}\text{Fe}_{70}$),⁵ which was reported to be ferromagnetic (FM) having $\sim 1\text{T}$ magnetization,^{7,8} this phase is believed to behave as the pinning phase due to its soft magnetism compared with the $\text{Nd}_2\text{Fe}_{14}\text{B}$ grains.⁵ However, further large pinning effect is anticipated if the magnetization of this pinning layer is able to be decreased.

Recently, for realizing the above idea, the slight amount of doping of Ga atoms into Nd-Fe-B magnets has been paid much attention. The doped Ga infiltrates into the GB phase preferentially,⁹ and, after optimal annealing, the GB phase has a tetragonal ordered $\text{Nd}_6\text{Fe}_{14-x}\text{Ga}_x$ phase^{10,11} belonging to $I4/mcm$ space group, which is presumed to be the changed structure from the amorphous $\text{Nd}_{30}\text{Fe}_{70}$ induced by the doped Ga. In addition, this ordered $\text{Nd}_6\text{Fe}_{14-x}\text{Ga}_x$ ($x = 1, 2$) forms an anti-ferromagnetic (AF) state,^{12,13} which is totally different from the FM state of the amorphous $\text{Nd}_{30}\text{Fe}_{70}$.

After this magnetic change, the pinning effect of DW at the GB phase is expected to increase because of its lower magnetization. In fact, after post-sintered optimal annealing, the enhancement of H_c in Ga doped Nd-Fe-B magnets have been observed to reach 80% ,¹¹ which considerably exceeds the conventional value in Ga non-doped systems $\simeq 20\%$.⁶

As mentioned above, one of the key factors for improving H_c in Nd-Fe-B magnets is to control the magnetic properties of the Fe-rich phase in the GB. For addressing this task, it is worth understanding the mechanism of the magnetic change from the FM state in the amorphous $\text{Nd}_{30}\text{Fe}_{70}$ phase to the AF state in the crystalline ordered $\text{Nd}_6\text{Fe}_{13}\text{Ga}$ phase. However, there exists few studies investigating the magnetic properties of these systems systematically, especially in the ordered phase. In the present study, we investigate magnetic properties of both the amorphous and the ordered Fe-rich $\text{Nd}_{30}(\text{Fe}, \text{Ga})_{70}$ alloys using first-principles methods. By considering the above observed magnetic change, our study concentrates on the effect on the stable magnetic structure of the $\text{Nd}_{30}(\text{Fe}, \text{Ga})_{70}$ systems by the structure change from amorphous to the ordered phase and the small amount of Ga doping.

Our main result is that the AF state in Fe-rich $\text{Nd}_{30}(\text{Fe}, \text{Ga})_{70}$ is realized only in the condition of both crystalline ordered structure and Ga doping. We also revealed that this stable AF state originates from the anti-parallel magnetic couplings between different Nd-Fe blocks in the ordered structure shown in Fig. 2 and doped Ga contributes to stabilizing this magnetic state.

The present paper is organized as follows. In Section II, our calculation methods and the considered crystal and magnetic structures for the Fe-rich $\text{Nd}_{30}(\text{Fe}, \text{Ga})_{70}$ systems are presented. Section III shows the calculated result for stable magnetic states of the amorphous $\text{Nd}_{30}\text{Fe}_{70-x}\text{Ga}_x$ and the ordered $\text{Nd}_6\text{Fe}_{14-x}\text{Ga}_x$. In Section IV, we discuss the origin of the obtained stable magnetic state in the ordered $\text{Nd}_6\text{Fe}_{14-x}\text{Ga}_x$ ($x = 0, 1$), which shows the AF state only in the Ga doped case

($x = 1$); this AF state is important to promote the pinning effect of DW at the GB in Nd-Fe-B magnets.

II. CALCULATION MODEL AND METHOD

In the amorphous phase, because of the difficulty in treating random atomic positions, we hypothesized the fcc lattice to reflect the short-range atomic correlation in an amorphous phase. Sakuma *et al.*⁸ demonstrated that the magnetism of the amorphous Nd-Fe alloys was successfully reproduced by the substitutional fcc disordered alloy. This hypothesis is based on the dense random packing of the hard-sphere model proposed by Yu *et al.*¹⁴, and many experiments suggested that the amorphous transition metals exhibit short-range order of closed packed structure like fcc. For treating the substitutional ternary disordered $\text{Nd}_{30}\text{Fe}_{70-x}\text{Ga}_x$ system, which has too many considerable atom alignments, we applied the coherent potential approximation (CPA), in which we replace randomly located atoms by effective $\text{Nd}_{30}\text{Fe}_{70-x}\text{Ga}_x$ atoms involving scattering effects as shown in Fig. 1. Within this CPA, we employed the tight-binding linear muffin-tin orbital method (TB-LMTO) under the local spin density functional approximation (LSDA)¹⁵ as the first-principles calculation method for the disordered $\text{Nd}_{30}\text{Fe}_{70-x}\text{Ga}_x$ alloys. The stable magnetic state of this amorphous system was judged by the sign of effective exchange interaction acting on an Fe magnetic moment at a certain site (0-site) defined by $J_0 = \sum_{i \neq 0} J_{i,0}$, where $J_{i,0}$ represents the strength of the exchange coupling between i and 0 sites. This $J_{i,0}$ was evaluated within the magnetic force theorem formulated by Lichtenstein *et al.*¹⁶ The obtained $J_0 > 0$ denotes the preference of the FM state over other magnetic structures.

The unit cell of the ordered $\text{Nd}_6\text{Fe}_{14-x}\text{Ga}_x$ ($x = 0, 1$) system consists of 80 atoms, as shown in Fig. 2. Because of few reports about the atomic position of $\text{Nd}_6\text{Fe}_{14}$ and $\text{Nd}_6\text{Fe}_{13}\text{Ga}$, we adopted atomic positions of $\text{Nd}_6\text{Fe}_{13}\text{Si}$ alloys¹⁷ alternatively. When $x = 1$, the doped Ga atoms were defined to replace the Fe layer in Fig. 2 on the basis of the experimental result.^{12,13} We adopted the displayed FM and AF states as candidates of stable magnetic states in the ordered system. The characteristic magnetic structure of the AF state is based on the observed one in $\text{Nd}_2\text{Fe}_{12}\text{Ga}_2$ alloys in the previous experiment.¹³ In both states, magnetic moments of internal atoms in the Nd-Fe blocks and Fe(Ga) layers are parallel as drawn by the thick arrow in Fig. 2, and magnetic moments of the adjacent Nd-Fe block and Fe(Ga) layer are, respectively, parallel in the FM state and parallel and anti-parallel in a ratio of 1:1 in the AF state. The stable magnetic state is determined by a direct comparison of the total energy between the FM and AF states. We used the Vienna ab initio simulation package (VASP 4.6) as a first-principles calculation method for obtaining the total energy. In this calculation, the self-consistent electronic structure

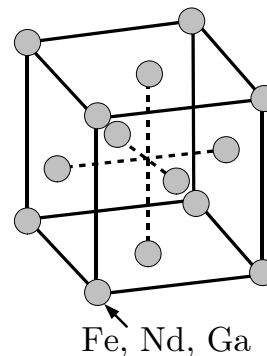


FIG. 1. Hypothesized disordered fcc structure for amorphous $\text{Nd}_{30}\text{Fe}_{70-x}\text{Ga}_x$.

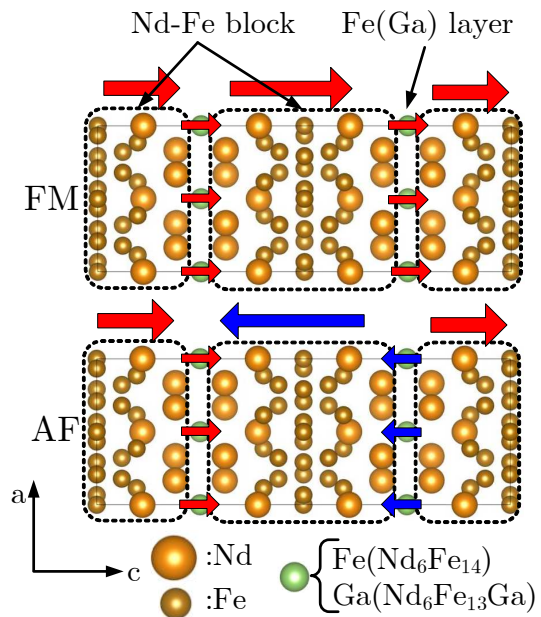


FIG. 2. Unit cell and candidates of stable magnetic structures of ordered $\text{Nd}_6\text{Fe}_{14}$ and $\text{Nd}_6\text{Fe}_{13}\text{Ga}$. The employed atomic positions are the observed value of $\text{Nd}_6\text{Fe}_{13}\text{Si}$ in the previous experiment.¹⁷

is obtained for valence electrons except for the $4f$ electrons in the Nd atoms, which were treated as core electrons in this study. The ionic potentials are described by the plane-augmented-wave (PAW) method,¹⁸ and the exchange-correlation energy of the valence electrons is represented within the generalized gradient approximation (GGA), whose specific form is given by Ceperly and Alder and parametrized by Perdew *et al.*¹⁹

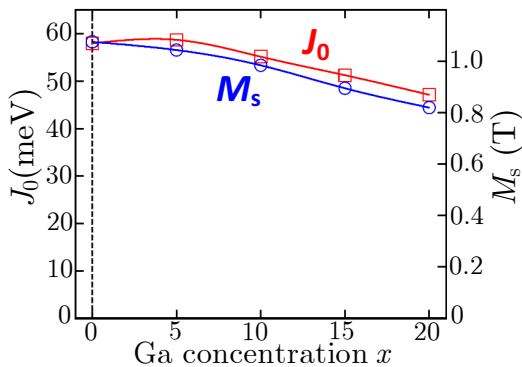


FIG. 3. Exchange coupling constant J_0 and saturation magnetization M_s as a function of Ga atom concentration x in the amorphous $\text{Nd}_{30}\text{Fe}_{70-x}\text{Ga}_x$.

III. CALCULATION RESULTS

First, we discuss the stable magnetic state of amorphous $\text{Nd}_{30}\text{Fe}_{70-x}\text{Ga}_x$. Figure 3 displays the exchange coupling energy J_0 acting on the Fe magnetic moment at a certain site as a function of the Ga concentration x . A positive J_0 value means that the FM state is a more stable state than the others. The saturation magnetization M_s of the FM state in each x condition is also shown. In $\text{Nd}_{30}\text{Fe}_{70}$, the obtained J_0 is almost 60 meV per atom, which denotes a preference for the FM state, in line with the previous studies.^{7,8} This stable state is attributed to its lattice constant, which is larger than that of fcc Fe owing to the addition of Nd atoms, as pointed out in a previous study.⁸ From the obtained $J_0 \simeq 60$ meV, we can roughly estimate the difference of energy between the FM and AF states to be around 120 meV per atom. This value was confirmed to be similar to the previous result approximately 100 meV,⁸ which was obtained from a direct comparison of the energy between the FM and AF states. When we look at the Ga doping case ($x > 0$), J_0 gradually decreases with increasing x . This decline is simply understood by the increased concentration of the non-magnetic Ga atom, which also attenuates M_s as displayed. However, the reduction of J_0 is slow against x , and $\text{Nd}_{30}\text{Fe}_{70-x}\text{Ga}_x$ is expected to maintain the FM state even if $x \simeq 20$. We conclude that the amorphous $\text{Nd}_{30}\text{Fe}_{70-x}\text{Ga}_x$ system keeps the FM state regardless of the level of Ga doping.

Next, we assess the stable magnetic state in the ordered $\text{Nd}_6\text{Fe}_{14}$ and $\text{Nd}_6\text{Fe}_{13}\text{Ga}$ system. Figure 4 shows the calculated energy of the FM and AF states in the unit cell of $\text{Nd}_6\text{Fe}_{13}\text{Ga}$ as a function of the lattice constant along the c -axis, c . The lattice constants along a - and b -axes were set as $a = b = 8.07$ Å from the experimental results of $\text{Nd}_{6.1}\text{Fe}_{13}\text{Ga}$.¹² The equilibrium c value is about 22.6 Å in this calculation; this value is almost equal to c of the above $\text{Nd}_{6.1}\text{Fe}_{13}\text{Ga}$ ¹² ($c = 22.9$ Å). One can find that, near the equilibrium c , the AF state has an energy

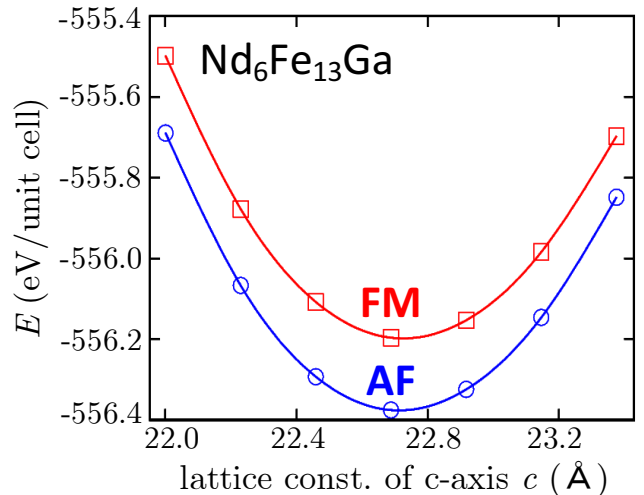


FIG. 4. Energy dependence of the FM and AF states in $\text{Nd}_6\text{Fe}_{13}\text{Ga}$ on the lattice constant along the c -axis, c .

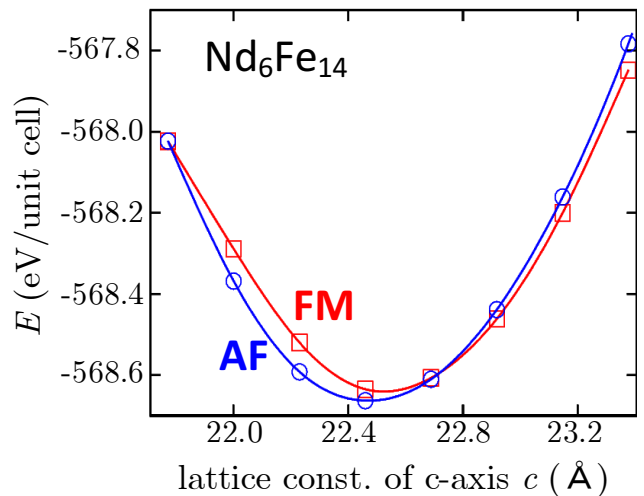


FIG. 5. Energy dependence of the FM and AF state in $\text{Nd}_6\text{Fe}_{14}$ on the lattice constant along the c -axis, c .

lower by 0.2 eV than that of the FM state; this preference for the AF state is consistent with the experimental results.^{12,13} It should be noted that the energy difference between the FM and AF states in the ordered phase ($\simeq 0.2$ eV/(80 atoms)) is quite small compared with the result of amorphous $\text{Nd}_{30}\text{Fe}_{70-x}\text{Ga}_x$ ($x \leq 20$) ($\simeq 0.1$ eV/(1 atom)). This small energy difference is attributed to the characteristic magnetic structure of the presumed FM and AF states in the ordered $\text{Nd}_6\text{Fe}_{14-x}\text{Ga}_x$, where the magnetic moments within each Nd-Fe block are parallel in the both states, as shown in Fig. 2.

The same comparison of energy for the unit cell of ordered $\text{Nd}_6\text{Fe}_{14}$ is shown in Fig. 5. The fixed value of a, b are common with the $\text{Nd}_6\text{Fe}_{13}\text{Ga}$ case, and the resultant

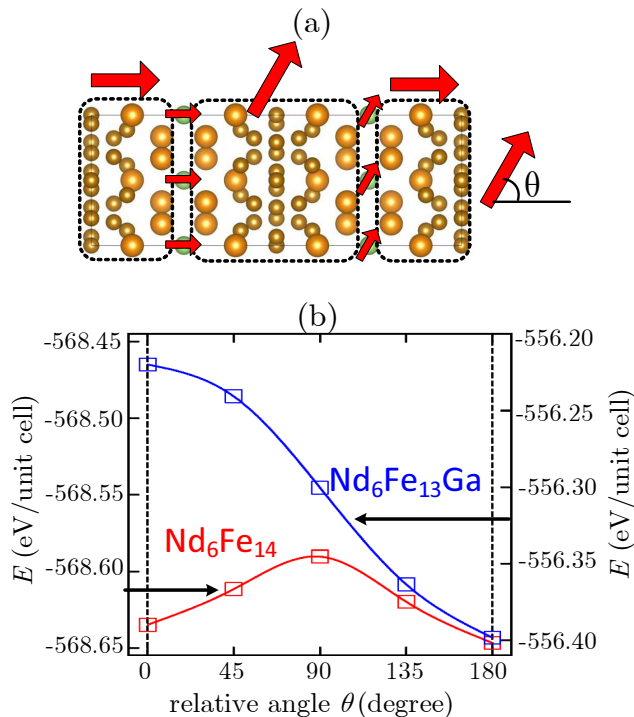


FIG. 6. (a) Our considered magnetic configuration, where the magnetic moments in half of the Nd-Fe blocks and Fe(Ga) layers have a relative angle θ with the magnetic moments of others. (b) Calculated energy in the condition of θ in $\text{Nd}_6\text{Fe}_{14}$ and $\text{Nd}_6\text{Fe}_{13}\text{Ga}$.

equilibrium c has a value similar to that of $\text{Nd}_6\text{Fe}_{13}\text{Ga}$. For the stable magnetic state, we found that the FM and AF states have almost the same energy (a difference of <0.01 eV) around the equilibrium c . This difference is so small compared with the result of $\text{Nd}_6\text{Fe}_{13}\text{Ga}$, and it is hard to identify the magnetic stable state in $\text{Nd}_6\text{Fe}_{14}$.

For further understanding of the energetic relationship between the two magnetic states in $\text{Nd}_6\text{Fe}_{14-x}\text{Ga}_x$ ($x = 0, 1$), we calculated the energy of each crystal in the case where magnetic moments continuously change from the FM state to the AF state. Figure 6(a) describes our considered non-collinear magnetic structure, where magnetic moments in half of the Nd-Fe blocks and Fe(Ga) layers rotate by an angle θ from those in the others. The obtained energy of $\text{Nd}_6\text{Fe}_{14-x}\text{Ga}_x$ ($x = 0, 1$) in each θ case is shown in Fig. 6(b). The cases of $\theta = 0^\circ$ and $\theta = 180^\circ$ correspond to the FM state and the AF state, respectively. The lattice constant of each structure was set as the value of each equilibrium point in Fig. 4 ($\text{Nd}_6\text{Fe}_{13}\text{Ga}$) and 5 ($\text{Nd}_6\text{Fe}_{14}$). In $\text{Nd}_6\text{Fe}_{13}\text{Ga}$, the AF state ($\theta = 180^\circ$) and the FM state ($\theta = 0^\circ$) correspond to the minimum and maximum energy point, respectively, and the magnetic energy monotonically becomes stable with increasing θ . In contrast, the maximum point in the case of $\text{Nd}_6\text{Fe}_{14}$ exists near $\theta = 90^\circ$, and double local minimum points are found near $\theta = 0^\circ$

TABLE I. Total magnetic moment (μ_B) in the unit cell of $\text{Nd}_6\text{Fe}_{14-x}\text{Ga}_x$ alloys ($x = 0, 1$) and local magnetic moment (μ_B) of the Nd-Fe blocks and the Fe(Ga) layers in the FM and AF states. The symbol \pm in the AF state represents the opposite direction of the magnetic moments between the two Nd-Fe blocks and between the two Fe(Ga) layers in the unit cell, as shown in Fig. 2.

$\text{Nd}_6\text{Fe}_{14}$	FM	AF
total	119.7	0.0
Nd-Fe block	55.0	± 56.5
Fe layer	4.9	± 4.9

$\text{Nd}_6\text{Fe}_{13}\text{Ga}$	FM	AF
total	112.8	0.0
Nd-Fe block	56.3	± 56.7
Ga layer	0.1	± 0.0

and $\theta = 180^\circ$. Two such stable points having almost the same energy will make the magnetic structure of $\text{Nd}_6\text{Fe}_{14}$ unstable. From these results, we conclude that doping of Ga atom significantly contributes to stabilizing the magnetic state of $\text{Nd}_6\text{Fe}_{14-x}\text{Ga}_x$ to the AF state. This remarkable effect of the doped Ga is specific to the ordered $\text{Nd}_6\text{Fe}_{14-x}\text{Ga}_x$ system, whereas, seldom appears in the amorphous $\text{Nd}_{30}\text{Fe}_{70-x}\text{Ga}_x$ system, as shown in Fig. 3.

IV. DISCUSSION FOR THE STABLE MAGNETIC STATE IN $\text{Nd}_6(\text{Fe}, \text{Ga})_{14}$

As shown in Section III, in the ordered $\text{Nd}_6\text{Fe}_{14-x}\text{Ga}_x$ system, the slight doping of Ga ($x = 1$) significantly contributes to realizing the AF state, which is expected to enhance the pinning effect of DW at the GB in Nd-Fe-B magnets. In this section, we discuss the dominant factors stabilizing the magnetic structure in $x = 0$ and $x = 1$ cases of the $\text{Nd}_6\text{Fe}_{14-x}\text{Ga}_x$ ($x = 0, 1$) system, focusing on the different magnetic properties between the Fe layer ($x = 0$) and the Ga layer ($x = 1$).

First, in Table I, we present the total magnetic moment in the unit cell in Fig. 2 and the local magnetic moment of each Nd-Fe block and Fe(Ga) layer in the FM and AF states of $\text{Nd}_6\text{Fe}_{14-x}\text{Ga}_x$ ($x = 0, 1$). The total magnetic moment consists of the two Nd-Fe blocks and the two Fe(Ga) layers. Note that the contribution from $4f$ electron in the Nd atoms, which were treated as core electrons in our calculation, are not considered in this table. In the FM state, the total magnetic moment of each alloy exceeds $110\mu_B$ per unit cell. For the contributions from the Nd-Fe blocks and the Fe(Ga) layers, one can find that the magnetic moments of the Ga layer in $\text{Nd}_6\text{Fe}_{13}\text{Ga}$ are almost zero regardless of the magnetic states. This result means that the magnetic couplings related to the Ga layers in $\text{Nd}_6\text{Fe}_{13}\text{Ga}$ can be disregarded.

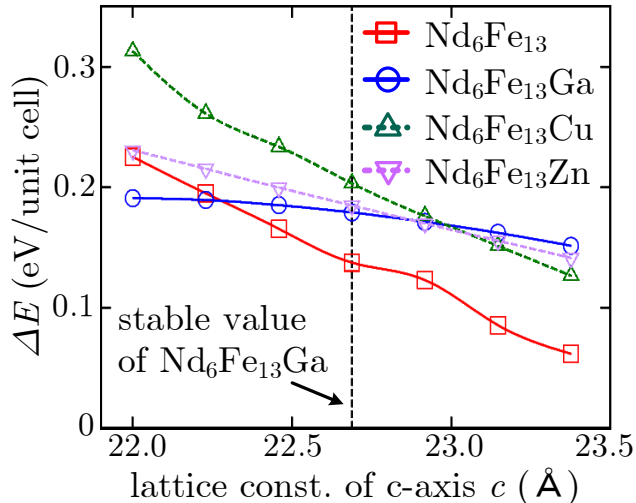


FIG. 7. Difference of energy between the FM and AF states $\Delta E = E(\text{FM}) - E(\text{AF})$ as a function of the lattice constant along the c-axis, c , in $\text{Nd}_6\text{Fe}_{13}\text{M}$ (where $\text{M} = \text{empty, Ga, Cu, or Zn}$).

In the $\text{Nd}_6\text{Fe}_{14-x}\text{Ga}_x$ system in Fig. 2, origin of the energy difference between the FM and AF states can be summarized as the magnetic couplings among different Nd-Fe blocks and different Fe(Ga) layers, since the relative angles among them characterize the difference of magnetic structure between the two states. Moreover, in $\text{Nd}_6\text{Fe}_{13}\text{Ga}$, this origin for the energy difference are expected to be reduced to the magnetic coupling only between the different Nd-Fe blocks because of the little magnetism in Ga layers as shown in table I.

To demonstrate the above hypothesis that the stable AF state in $\text{Nd}_6\text{Fe}_{13}\text{Ga}$ mainly originates from the magnetic couplings between the different Nd-Fe blocks, we presumed the structure $\text{Nd}_6\text{Fe}_{13}$, where the Ga layers in $\text{Nd}_6\text{Fe}_{13}\text{Ga}$ are replaced by the vacancies with the locations of other sites fixed, and we compared the stability of the AF state between $\text{Nd}_6\text{Fe}_{13}\text{Ga}$ and $\text{Nd}_6\text{Fe}_{13}$. In Fig. 7, the energy differences between the FM state and the AF state ($\Delta E = E(\text{FM}) - E(\text{AF})$) are displayed as a function of the lattice constant along the c-axis, c , whose value is around the equilibrium value in $\text{Nd}_6\text{Fe}_{13}\text{Ga}$ in Fig. 4. The lattice constants along the a- and b-axes were also set to the values used in Fig. 4. A positive (negative) ΔE denotes the preference of the AF (FM) state. The results of $\text{Nd}_6\text{Fe}_{13}$ and $\text{Nd}_6\text{Fe}_{13}\text{Ga}$ are represented by the red and blue solid lines, respectively. For comparison, the results of $\text{Nd}_6\text{Fe}_{13}\text{Cu}$ (Zn), where the Ga atoms in $\text{Nd}_6\text{Fe}_{13}\text{Ga}$ are replaced by Cu (Zn) atoms having two (one) fewer electrons than Ga, is also shown as the green (purple) dashed line. We found that all of these alloys including $\text{Nd}_6\text{Fe}_{13}$ favor the AF state over the FM state. In addition, near the equilibrium c of $\text{Nd}_6\text{Fe}_{13}\text{Ga}$, ΔE of $\text{Nd}_6\text{Fe}_{13}\text{Ga}$ has a value similar

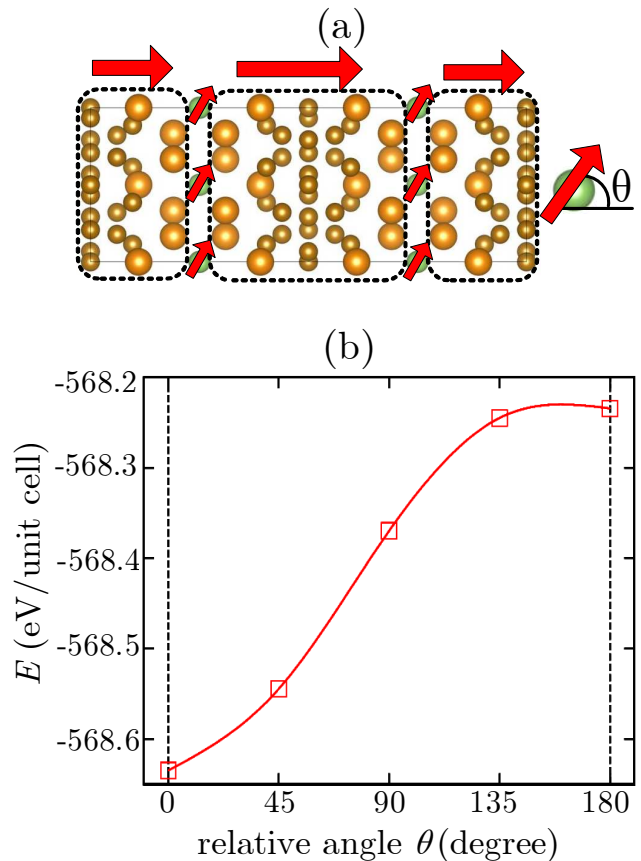


FIG. 8. (a): Assumed magnetic structure in $\text{Nd}_6\text{Fe}_{14}$, where the magnetic moments in the Fe layer have a relative angle θ with those in the Nd-Fe blocks. (b): Calculated energy as a function of θ .

to that of $\text{Nd}_6\text{Fe}_{13}$. From this result, we conclude that the stability of the AF state in $\text{Nd}_6\text{Fe}_{13}\text{Ga}$ mainly originates from the anti-parallel magnetic coupling between the neighboring Nd-Fe blocks and has little relation to the Ga layers. The similar ΔE values between $\text{Nd}_6\text{Fe}_{13}$ and $\text{Nd}_6\text{Fe}_{13}\text{Cu}$ and $\text{Nd}_6\text{Fe}_{13}\text{Zn}$ alloys also support our above interpretation. In addition, from ΔE value in $\text{Nd}_6\text{Fe}_{13}$, we can estimate the energetic preference of the AF state induced by the above anti-parallel coupling in the $\text{Nd}_6(\text{Fe, Ga})_{14}$ system as $\Delta E_{\text{Nd-Fe/Nd-Fe}} = E(\text{AF})_{\text{Nd-Fe/Nd-Fe}} - E(\text{FM})_{\text{Nd-Fe/Nd-Fe}} \simeq -0.2\text{eV}$ per unit cell.

To discuss the dominant factor of the stable magnetic state in $\text{Nd}_6\text{Fe}_{14}$, we further paid attention to the magnetic interactions between the Nd-Fe blocks and the Fe layers, which have finite magnetism different from the Ga layers. To evaluate the magnetic energy induced from these interactions, we assumed the non-collinear magnetic configuration as shown in Fig. 8(a), where the magnetic moments in the Fe layers rotate by an angle θ from those of the Nd-Fe blocks. Figure 8(b) presents the energy dependence of $\text{Nd}_6\text{Fe}_{14}$ on the above θ . The

used lattice constants were those of the equilibrium point in Fig. 5, and the condition of $\theta = 0^\circ$ corresponds to the FM state in Fig. 2. We found that the calculated energy monotonically increases with increasing θ ; this result indicates parallel magnetic couplings between the Nd-Fe blocks and Fe layers. These parallel couplings realize between all neighboring Nd-Fe block and Fe layer in the FM state, whereas in the AF state shown in Fig. 2, there exist both parallel and anti-parallel couplings between the neighboring Nd-Fe block and Fe layer in a ratio of 1:1 in the unit cell. The energetic instability of the AF state originating from these anti-parallel couplings in $\text{Nd}_6\text{Fe}_{14}$ is estimated as $\Delta E_{\text{Nd-Fe/Fe}} = E(\text{AF})_{\text{Nd-Fe/Fe}} - E(\text{FM})_{\text{Nd-Fe/Fe}} \simeq 0.2\text{eV}$ per unit cell, which is half of the energy difference between $\theta = 0^\circ$ and $\theta = 180^\circ \simeq 0.4\text{eV}$ per unit cell in Fig. 8(b). One can find that this $\Delta E_{\text{Nd-Fe/Fe}}$ value almost cancels out with the other $\Delta E_{\text{Nd-Fe/Nd-Fe}} \simeq -0.2\text{eV}$ per unit cell derived from Fig. 7, which arises from the anti-parallel couplings between the neighboring Nd-Fe blocks in the $\text{Nd}_6\text{Fe}_{14-x}\text{Ga}_x$ system. We conclude that this energetic balance between the two ΔE might induce the double local minimum points of the magnetic states in $\text{Nd}_6\text{Fe}_{14}$ as shown in Fig. 6(b), whereas, $\text{Nd}_6\text{Fe}_{13}\text{Ga}$ has the AF single stable state because only $\Delta E_{\text{Nd-Fe,Nd-Fe}}$ has considerable effects.

V. SUMMARY

To understand magnetism of the GBs in Nd-Fe-B magnets, which is believed to contribute to the pinning effect on DW motion in the magnetization reversal process, we investigated the magnetic properties of Fe-rich Nd(Fe,Ga) alloys using the first-principles technique. Our study concentrated on the contributions of both (1) the amorphous ordered structure change and (2) the doping of Ga atoms to the stable magnetic struc-

ture of Fe-rich Nd(Fe,Ga), which was observed to change from the FM state to the AF state after both (1) and (2) operations in experiments. The research target was the amorphous $\text{Nd}_{30}\text{Fe}_{70-x}\text{Ga}_x$, which was hypothesized to have fcc structure, and the ordered $\text{Nd}_6\text{Fe}_{14-x}\text{Ga}_x$.

It was demonstrated that the amorphous $\text{Nd}_{30}\text{Fe}_{70-x}\text{Ga}_x$ keeps the FM state regardless of the level of Ga doping ($x \leq 20$). In contrast, the magnetic state of the ordered $\text{Nd}_6\text{Fe}_{14-x}\text{Ga}_x$ was found to be sensitive to small x . In $\text{Nd}_6\text{Fe}_{14}$ ($x = 0$), the stable magnetic structure was suggested to be unstable because of the too small energy difference between the FM and AF state (≤ 0.01 eV per unit cell), whereas in $\text{Nd}_6\text{Fe}_{13}\text{Ga}$ ($x = 1$), the AF state became an only stable state having an energy lower by ~ 0.2 eV per unit cell than that of the FM state.

Furthermore, we discussed the mechanism of the magnetic change from the FM state in the amorphous $\text{Nd}_{30}\text{Fe}_{70}$ to the AF state in the ordered $\text{Nd}_6\text{Fe}_{13}\text{Ga}$. First, the structure change from the amorphous to the ordered phase makes the Nd-Fe blocks in Fig. 2, which prefer the anti-parallel magnetic couplings between the neighboring Nd-Fe blocks. Second, the doped Ga helps to realize the above anti-parallel couplings by substituting Fe atoms, whose magnetic interaction favors the parallel couplings between the neighboring Nd-Fe blocks.

Consequently, we revealed that both the structure change into the ordered phase and the Ga doping are indispensable factor for obtaining the AF state in Fe-rich Nd(Fe,Ga) alloys.

ACKNOWLEDGMENTS

This work was supported by JST-CREST. Private communications with T. T. Sasaki and S. Doi are also appreciated.

-
- ¹ K. Hono and H. Sepehri-Amin, *Scr. Mater.* **67**, 530 (2012).
 - ² J. Liu, H. Sepehri-Amin, T. Ohkubo, K. Hioki, A. Hattori, T. Schrefl, and K. Hono, *Acta Mater.* **82**, 336 (2015).
 - ³ R. K. Mishra, J. K. Chen, and G. Thomas, *J. Appl. Phys.* **59**, 2244 (1986).
 - ⁴ F. Vial, F. Joly, E. Nevalainen, M. Sagawa, K. Hiraga, and K. Park, *J. Magn. Magn. Mater.* **242**, 1329 (2002).
 - ⁵ H. Sepehri-Amin, T. Ohkubo, T. Shima, and K. Hono, *Acta Mater.* **60**, 819 (2012).
 - ⁶ W. Li, T. Ohkubo, and K. Hono, *Acta Mater.* **57**, 1337 (2009).
 - ⁷ Y. Murakami, T. Tanigaki, T. Sasaki, Y. Takeno, H. Park, T. Matsuda, T. Ohkubo, K. Hono, and D. Shindo, *Acta Mater.* **71**, 370 (2014).
 - ⁸ A. Sakuma, T. Suzuki, T. Furuuchi, T. Shima, and K. Hono, *Apex* **9**, 013002 (2016).
 - ⁹ J. Fidler, C. Groiss, and M. Tokunaga, *IEEE Trans. Magn.* **26**, 1948 (1990).
 - ¹⁰ J. Bernardi, J. Fidler, M. Seeger, and H. Kronmuller, *IEEE Trans. Magn.* **29**, 2773 (1993).
 - ¹¹ T. Sasaki, T. Ohkubo, Y. Takada, T. Sato, A. Kato, Y. Kaneko, and K. Hono, *Scr. Mater.* **113**, 218 (2016).
 - ¹² C. H. de Groot, K. H. J. Buschow, and F. R. de Boer, *Phys. Rev. B* **57**, 11472 (1998).
 - ¹³ P. Schobinger-Papamantellos, K. Buschow, and C. Ritter, *J. Alloys. Compd.* **359**, 10 (2003).
 - ¹⁴ M. Yu, Y. Kakehashi, and H. Tanaka, *Phys. Rev. B* **49**, 352 (1994).
 - ¹⁵ I. Turek, V. Drchal, J. Kudrnovský, M. Sob, and P. Weinberger, *Electronic Structure of Disordered Alloys, Surfaces and Interfaces*, 1997th ed. (Springer, 1996).
 - ¹⁶ A. Liechtenstein, M. Katsnelson, V. Antropov, and V. Gubanov, *J. Magn. Magn. Mater.* **67**, 65 (1987).
 - ¹⁷ J. Allemand, A. Letant, J. Moreau, J. Nozieres, and R. D. L. Bathie, *J. Less Common Met.* **166**, 73 (1990).
 - ¹⁸ P. E. Blöchl, *Phys. Rev. B* **50**, 17953 (1994).

¹⁹ J. P. Perdew, J. A. Chevary, S. H. Vosko, K. A. Jackson,

M. R. Pederson, D. J. Singh, and C. Fiolhais, Phys. Rev. B **46**, 6671 (1992).